e-ISSN 2320 –7876 www.ijfans.org
Vol.11, Iss.6, 2022
Research Paper © 2012 IJFANS. All Rights Reserved, **UGC CARE Listed (Group -I) Journal**

Synthesis, Characterization And Biomedical Application Of Iron Nanoparticles Synthesized From Vernonia Cinerea

Mary Jency. J[1*]

[1]Reg.No: 20113012032001, Department of Chemistry, Annai Velankanni College, Tholayavattam, Kanyakumari District, TamilNadu
[1]Affiliated to Manonmaniam Sundaranar University, Tirunelveli – 627 012.

Brintha. S. R[2]

[2]Associate Professor, Department of Chemistry, Annai Velankanni College, Tholayavattam, Kanyakumari District, TamilNadu

***Corresponding Author:** Brintha. S. R

Associate Professor, Department of Chemistry, Annai Velankanni College, Tholayavattam, Kanyakumari District, TamilNadu

Abstract
The present study was undertaken to the *in-vitro* antioxidant properties of *Vernonia cinerea* and to synthesis, characterization and evaluate the biomedical application of iron nanoparticles from *V. cinerea.* For this *V. cinerea* was collected and the leaves were extracted using different solvents (ethanol, hexane, chloroform). Further the antioxidant potential of various concentrations (100 to 300µg/ml) of the extracts was performed through different standard antioxidant assays. The antioxidant potential of the extracts was compared with standard ascorbic acid. Iron nanoparticles were synthesized using *V. cinerea* leaf extract. The formation of iron nanoparticles was confirmed by characterization such as UV–vis spectroscopy, Fourier transform infra-red spectroscopy (FTIR), X-ray diffraction (XRD), Scanning electron microscope (SEM) and Energy dispersive X-ray analysis (EDAX) analysis. The anticancer activity of synthesized iron nanoparticles was evaluated against human lung cancer (A549) cells and human colon cancer (HCT-116) cell line.

The highest antioxidant activity was observed for ethanol extract with 72.67% DPPH radical scavenging activity, hexane extract with 87.60% superoxide scavenging activity, and chloroform extract with 57.63% hydroxyl radical scavenging activity, all at a concentration of 300 µg/mL. These results indicate that *V. cinerea* possesses significant antioxidant potential, particularly at higher concentrations. The formation of iron nanoparticles was observed by a colour change to brown and confirmed by UV spectral_analysis, which showed peak at 268 nm. FTIR analysis indicated the involvement of various functional groups, such as carboxylic acids, aromatics, and amines, in the nanoparticle formation. XRD analysis revealed the presence of iron nanoparticles with a peak at 53 nm. SEM and EDAX images revealed that iron nanoparticles to be approximately 1-5 nm in size. Anticancer activity of iron nanoparticles showed better growth inhibition of A549 cells and HCT-116 cell lines at the maximum concentration of 150µg/ml, when compared to that of the standard drug cisplatin and fluorouracil. Future research should further explore the potential applications of iron nanoparticles synthesized from *V. cinerea* extract and investigate their environmental and biomedical implications.

Keywords: *Vernonia cinerea*, iron nanoparticles, anticancer activity.

Research Paper © 2012 IJFANS. All Rights Reserved, **UGC CARE Listed (Group -I) Journal**

1. Introduction

Medicinal plants are generally used in curing specific diseases and are believed to be helpful in maintaining good health. More than 80% of people in the world depend largely on herbal medicines for their basic health care requirements (Okigbo *et al.,* 2009). Iron nanoparticles (FeNPs) are the tiniest particle of iron metal with a large surface area and high reactivity. They are non-toxic. FeNPs have excellent dimensional stability and also possess high thermal and electrical conductivity, high surface area and are highly magnetic. FeNPs can oxidize immediately when exposed to water or air and produces free Fe ions. There are numerous applications of FeNPs such as magnetic and electrical applications and biomedical applications, which include the labeling and magnetic separation of biological materials, directed drug delivery, MRI contrast enhancement and hyperthermia treatment (Pankhurst *et al.,* 2003). Biological biosynthesis of iron oxide nanoparticles is based upon the usage of living biota like plants, bacteria, algae, actinomycetes, viruses and fungi (Gahlawat and Choudhury, 2019). FeNPs are reported to be toxic to cancer cells because of their ROS generating ability. Various studies have been conducted on their ability to kill cancer cell in vitro and in vivo, alone or in combination with other therapeutic modalities (Markides *et al.,* 2012). FeNPs among other high-atomic number materials, are also being studied currently for their potential to increase the therapeutic efficacy of ionizing radiation (Vallabani and Singh, 2018) They can be used in MRI, targeted drug delivery to diseased tissues, magnetic hyperthermia based killing of diseased tissues (Polyak and Friedman, 2009) and radio sensitization (Huang and Hainfeld, 2013). The most important aspect of using FeNPs in biological application is that they undergo degradation and are assimilated in body metabolism, without accumulating or causing toxicity to the body (Zhao *et al.,* 2014).

Plants are generally considered as freely available, easy to handle, harmless and cheap material for synthesis of various types of nanoparticles (Noruzi, 2015). The usage of medicinal plant or herbal extracts for the synthesis of NPs incorporates the medicinal properties in the synthesized NPs (Rokade *et al.,* 2018). Plant mediated synthesis has been considered to be the most advantageous method for the synthesis of metal nanoparticles. Plant materials such as the stem, fruit, fruit peels, bark, root, and leaves can all be utilized to create NPs (Ramanathan and Aqra, 2019). India has one of the oldest, richest and most diverse cultural traditions associated with the consumer of medicinal plants.

Vernonia cinerea (L.) less is an important medicinal herb, belongs to the family Asteraceae and are considered among one of the most advanced family from the dicotyledons. Commonly called little iron weed or Sahdevi. *V. cinerea* is an annual herb, branched and slender-stemmed, the leaves are dark-green alternate spiral or elliptic. It is traditionally used as febrifuge, diaphoretic, diuretic, antispasmodic and anthelmintic (Khare, 2007). Various parts of the plant are reported to contain sterols such as stigmasterols, sitosterols and spinasterols; triterpenoids like amyrin and lupeol; sesquiterpenes, glycosides and flavonoids (Khare, 2007; Kuo *et al.,* 2003). Different parts of *V. cinerea* have been used in folk medicine applications and have been reported to possess medicinal properties. The seeds are useful in treating leucoderma and dysiria. The plant has anticancerous properties and is beneficial for cancerous malformations. It is alternative and purifies blood, piles and semen (Pullaih, 2002; Prajapathi *et al.,* 2003). The bioactive compounds of VC have been characterized and quantified using gas chromatography-mass spectrometry (GC/MS). Various phytochemical substances, including sterols, flavonoids, alkaloids, triterpenoids, sesquiterpenes and tannins, have been isolated from VC by GC/MS (Ansar *et al.,* 2017).

V. cinerea possesses significant antioxidant, antiradical and GABA enhancing effects against sunset yellow induced anxiogenic behaviour in mice (Krishnan *et al.,* 2021). The plants possess antimicrobial, antibacterial (Gupta *et al.,* 2003), antihelmentic, antiinflammatory, hepatoprotective), analgesic, antipyretic, antiflatulent, antispasmodic, antioxidant and anticholineesterase activities, antidiabetic, renoprotective, antiviral activities. *V. cinerea* extract play significant role in regulating inflammatory response and as an anticancer activity against various cell types such as colon adenocarcinoma, lung large carcinoma and hela tumour cell line (Pratheeshkumar and Kuttan, 2011). *V. cinerea* possesses potent antioxidant and anti-inflammatory properties, antimicrobial activity

against various pathogens (Divya Theja and Nirmala, 2023). The green synthesized silver nanoparticles from *V. cinerea* plant extract showed promising anticancer, antioxidant and anti-bacterial activities (Palei *et al.*, 2023).

Vernonia cinerea has not been explored much for synthesizing FeNPs. Therefore, considering the importance of the above, in present study, plant extract of *Vernonia cinerea* was used to synthesis the iron nanoparticles. The synthesised iron nanoparticles were characterised using UV-Vis spectrometer, FTIR spectrometer, XRD, EDX, and SEM. Moreover, medicinal applications will be supported from anticancer behaviour of the synthesized iron nanoparticles was studied.

2. Methodology

2.1. Preparation of leaf extract and biosynthesis of iron nanoparticles

V. cinerea were collected from Saral, Kanyakumari district, Tamilnadu. The authentication of the plant was done by Dr. Nagendra Prasad, Botanist, Retd Professor, Sri Paramakalyani College, Alwarkurichi. The leaves were rinsed with tap water and extracts were prepared. Leaf extracts were prepared by taking around 25 grams of leaves. The samples were carefully cleansed with distilled water, then dried and pulverized using a mixer. Finally, the powder was finely homogenized using a mortar and pestle. 2gm of plant extract was dissolved in 50ml of ethanol, hexane, chloroform and deionized water and stirred with a magnetic stirrer for three hours to get *V. cinerea* plant extract. For the synthesis of iron nanoparticles (Vc-FeNPs), The aqueous *V. cinerea* extract was filtered after an hour of stabilization. 10ml of 0.01 M $FeSO_4$ solution at 70°C was mixed with the filtrate. The solution was cooled and centrifuged at 10,000 rpm for 2 minutes. The product was dried in an oven at 50°C for 3 hours.

2.2. *In vitro* Antioxidant Activity of *V. cinerea*

2.2.1. 2,2-Diphenyl-1-picrylhydrazyl assay (DPPH)

The free radical scavenging activity of the fractions was measured *in vitro* by 2,2′- diphenyl-1-picrylhydrazyl (DPPH) assay according to the standard method. The stock solution was prepared by dissolving 24 mg DPPH with 100 ml of ethanol stored at 20°C until required. A working solution was obtained by diluting DPPH solution with ethanol and 3 ml aliquot of this solution was mixed with 1 ml of *V. cinerea* at different concentrations (100, 200, and 300 µg/mL) in various solvents (ethanol, hexane, chloroform). The reaction mixture was shaken well and incubated in the dark for 15 min at room temperature. Then the absorbance was taken at 517 nm. A control was prepared without any sample and scavenging activity was estimated based on the percentage of DPPH radical scavenging as the following equation.

$$Percentage\ of\ inhibition = \left[\frac{control\ OD - sample\ OD}{control\ OD}\right] \times 100$$

2.2.2. Superoxide anion scavenging activity

The assay for superoxide anion radical scavenging activity was supported by riboflavin-light-NBT system. 1 ml of *V. cinerea* at different concentrations (100, 200, and 300 µg/mL) in various solvents (ethanol, hexane, chloroform) was mixed with 0.1 ml of riboflavin solution (20 µg/ml), 0.2 ml of EDTA solution (12 mM), 0.2 ml of methanol and 0. 1 ml of Nitro-blue tetrazoliumn (0.5 mM) were mixed in a test tube. The reaction mixture was diluted up to 3 ml with phosphate buffer (50 mM). After 20 minutes of incubation at room temperature, the absorbance was measured at 560 nm. Ascorbic acid was used as standard.

The scavenging ability of the plant extract was determined by the following equation

$$\text{Scavenging activity (\%)} = \left[\frac{\text{control OD} - \text{sample OD}}{\text{control OD}}\right] \times 100$$

2.2.3. Hydroxyl radical scavenging activity

The reaction mixture contained 0.8 ml of phosphate buffer solution (50 mmol L^{-1}, pH 7.4), 0.2 ml of *V. cinerea* extract at different concentrations (100, 200, and 300 µg/mL) in various solvents (ethanol, hexane, chloroform), 0.2 ml of EDTA (1.04 mmol L^{-1}), 0.2 ml of $FeCl_3$(1 mmol L^{-1}), and 0.2 ml of 2-deoxyribose (60 mmol L^{-1}). The mixtures were kept in a water bath at 37°C and the reaction was started by adding 0.2 mL of ascorbic acid (2 mmol L^{-1}) and 0.2 ml of H_2O_2 (10 mmol L^{-1}). After incubation at 37 °C for 1 hour, 2 ml of cold thiobarbituric acid (10 g L^{-1}) was added to the reaction mixture followed by 2 ml of HCl (25%). The mixture was heated at 100°C for 15 minutes and then cooled down with water. The absorbance of solution was measured at 532 nm with a spectrophotometer. The hydroxyl radical scavenging capacity was evaluated with the inhibition percentage of 2-deoxyribose oxidation on hydroxyl radicals.

The scavenging percentage was calculated according to the following formula

$$\text{Scavenging activity } (\%) = \left[\frac{control\ OD - sample\ OD}{control\ OD}\right] \times 100$$

2.3. Characterization of iron nanoparticles

The size, elemental composition and morphology of FeNPs in *V. cineria* are analyzed using analytical methods such as UV-visible spectrophotometry (UV-Vis), Fourier Transform Infrared Spectroscopy (FTIR), Xray Diffraction analysis (XRD) and SEM-EDAX (Scanning Electron Microscope equipped with Energy Dispersive Xray analysis).

2.4. Anticancer activity

Human lung cancer (A549) cell and human colon cancer (HCT-116) cell lines were obtained from the National Centre for Cell Sciences (NCCS), Pune, India and maintained in a humidified atmospheric condition with 5% CO 2 at 37°C. All cell lines were routinely cultured individually in Dulbecco's modified Eagles medium (Gibco, Invitrogen), supplemented with 10% fetal bovine serum (FBS), 100 U/ml penicillin, 100 µg/ml streptomycin, 2.5µg/ml Amphoteracin B and 2 mML-glutamine. The viability of all the cell lines was evaluated by direct observation via inverted phase contrast microscope followed by MTT assay method. The logarithmically growing selected cell lines were plated individually in flat-bottom 96-well microplate at a density of 1 × 10 4 cells and cultured for 24 h. Then these cell lines were treated with Vc-FeNps separately at different concentrations (12.5, 25, 50, 100, 200µg/ml). After 24h of incubation, 100µl of 5mg/ml MTT solution [5 mg/ml in phosphate buffer saline (PBS)] was added in to each well. This is incubated in dark for 4 hrs in CO_2 incubator at 37ºC. After the incubation period, the supernatant was removed and 100µl of MTT Solubilization Solution (DMSO) was added and the wells were mixed gently by pipetting up and down in order to solubilize the formazan crystals. Absorbance was measured at 570 nm using a multi-well plate spectrophotometer. The results were calculated as the percentage of absorbance with respect to that of the control. Non-linear regression graph was plotted between percentage cell inhibition and log concentration and IC_{50} values were determined using GraphPad Prism 7 software. Control (untreated cells) was also maintained throughout the experiment. All experiments were performed in triplicate for each cell line. The results were compared with positive control (Cyclophosphamide treated cell lines). Images of all cancer cell lines treated groups were captured and quantified using a fluorescent microscope. The cell viability (%) was calculated according to the following formula

Calculation

$$\text{The percentage cell viaility } (\%) = \left[\frac{\text{Absorbance of test sample}}{\text{Absorbance of control}}\right] \times 100$$

$$\text{The percentage cell inhibition } (\%) = \left[\frac{100 - \text{Absorbance of test sample}}{\text{Absorbance of control}}\right] \times 100$$

3. Result

3.1. DPPH radical scavenging activity

The DPPH radical scavenging activity of *V. cinerea* extracts differed significantly depending on the solvent used. Hexane, chloroform and ethanol extracts exhibited the highest activity (67.407, 33.796 and 72.677%) at the highest (300µg/ml) concentration. Here, DPPH radical scavenging activity was increased with increasing concentrations of *V. cinerea* (Table.3.1). At the lowest concentration (100µg/ml), hexane (26.235 ± 0.513%), chloroform (9.75 ± 0.036%) and ethanol (37.033 ± 0.061%) displayed the minimum radical scavenging activity. At the same time, the DPPH radical scavenging activity of the standard drug ascorbic acid reached a maximum activity of 41.79% only at the highest concentration (300µg/ml). The IC_{50} values recorded were 214.932µg/ml, 418.51µg/ml and 163.496µg/ml for hexane, chloroform and ethanol respectively. However, the IC_{50} value observed for standard drug ascorbic acid was 458.875µg/ml (Table 3.1).

Table 3.1. *In vitro* DPPH radical scavenging activity of *V. cinerea* at different solvents and concentrations compared with standard ascorbic acid

Samples	Concentration of *V. cinerea*			IC_{50} Value
	100 µg/ ml	200 µg/ ml	300 µg/ ml	
Hexane	26.235 ± 0.513	47.136 ± 0.043	67.407 ± 0.016	214.932
Chloroform	9.75 ± 0.036	27.697 ± 0.109	33.796 ± 0.106	418.51
Ethanol	37.033 ± 0.061	59.807 ± 0.026	72.677 ± 0.041	163.496
Standard (Ascorbic acid)	31.18 ± 0.003	35.83 ± 0.002	41.79 ± 0.004	458.875

3.2. Superoxide radical scavenging activity

The *in vitro* superoxide radical scavenging activity of *V. cinerea* extracts varied significantly depending on the solvent used. Interestingly Hexane, chloroform and ethanol extracts exhibited the lowest activity (87.601 ± 0.004, 81.266 ± 0.018 and 6.064 ± 0.421%, respectively) at the highest (300µg/ml) concentration. However, superoxide radical scavenging activity was increased with increasing concentrations of *V. cinerea* (Table 3.2). At the lowest concentration (100µg/ml), hexane 99.679%), chloroform (99.445 ± 1.74%) and ethanol (65.137 ± 0.063%) displayed the maximum radical scavenging activity. At the same time, the superoxide radical scavenging activity of the standard drug ascorbic acid reached a maximum activity of 17.06% only at the highest concentration (300µg/ml). The IC_{50} values recorded were determined to be 916.962µg/ml, 670.697µg/ml and 119.774µg/ml for hexane, chloroform and ethanol extracts respectively. However, the IC_{50} value observed for standard drug ascorbic acid was 146.061µg/ml.

Table 3.2 *In vitro* superoxide radical scavenging activity of *V. cinerea* at different solvents and concentrations compared with standard ascorbic acid

Samples	Concentration of *V. cinerea*			IC_{50} Value
	100 µg/ ml	200 µg/ ml	300 µg/ ml	
Hexane	99.679 ± 0	92.612 ± 0.04	87.601 ± 0.004	916.962
Chloroform	99.445 ± 1.74	97.641 ± 0.011	81.266 ± 0.018	670.697
Ethanol	65.137 ± 0.063	8.744 ± 0.011	6.064 ± 0.421	119.774

Research Paper © 2012 IJFANS. All Rights Reserved, **UGC CARE Listed (Group -I) Journal**

Standard (Ascorbic acid)	62.762 ± 0.019	33.201 ± 0.02	17.06 ± 0.029	146.061

3.3. Hydroxyl radical scavenging activity

The result on hydroxyl radical scavenging activity of *V. cinerea* extracts varied depends on the solvent used. Hexane, chloroform and ethanol extracts possessed better activity (35.099, 33.561 and 57.637% respectively) at the highest (300µg/ml) concentration. Here, hydroxyl radical scavenging activity was decreased with increasing concentrations of *V. cinerea* (Table 3.3). At the lowest concentration (100µg/ml), hexane (63.98 ± 0.032%), Chloroform (49.268 ± 0.109%) and ethanol (95.412 ± 0.029%) showed the highest radical scavenging activity. At the same time, the hydroxyl radical scavenging activity of the standard drug ascorbic acid displayed 38.85% at the highest concentration of 300µg/ml. The IC_{50} values recorded were 319.023µg/ml, 326.64µg/ml and 328.634µg/ml for hexane, chloroform and ethanol respectively. However, the IC_{50} value observed for standard drug ascorbic acid was 237.444µg/ml.

Table 3.3. *In vitro* hydroxyl radical scavenging activity of *V. cinerea* at different solvents and concentrations compared with standard ascorbic acid

Samples	Concentration of *V. cinerea*			IC_{50} Value
	100 µg/ ml	200 µg/ ml	300 µg/ ml	
Hexane	63.98 ± 0.032	57.719 ± 0.059	35.099 ± 0.181	319.023
Chloroform	49.268 ± 0.109	37.334 ± 0.332	33.561 ± 0.43	326.64
Ethanol	95.412 ± 0.029	69.838 ± 0.009	57.637 ± 0.018	328.634
Standard (Ascorbic acid)	64.882 ± 0.25	60.889 ± 0.32	38.85 ± 0.035	237.444

3.4. Synthesis of FeNPs using *V. cinerea*

When 10 ml of aqueous extract of *V. cinerea* were added to 10 ml of $FeSO_4$. The colour changes of the solutions from green to dark brown indicated the reduction of Fe^{+3} ions in aqueous solution due to the excitation of surface plasmon vibrations in iron nanoparticles (Fig 3.1).

Fig. 3.1: Colour change of the reaction mixture from green to reddish brown indicates the formation of NPs (A) Aqueous *V. cinerea* extract; (B) Biosynthesized FeNPs suspension (dark reddish brown)

Research Paper © 2012 IJFANS. All Rights Reserved, **UGC CARE Listed (Group -I) Journal**

3.5. Characterizations of synthesis of nanoparticles using *V. cinerea*

3.5.1. UV-Vis Spectrophotometer

The UV-Vis spectrum analysis of the FeNPs show characteristic absorbance peaks due to the excitation mode of their surface plasmons resonance (SPR) of this nanoparticle. As a result, absorption peak at the wavelength of 268nm showed the presence of iron nanoparticles (Fig 3.2). Absorption at 268nm indicates the likely presence of smaller iron nanoparticles or iron oxide nanoparticles. Such nanoparticles typically display UV absorption due to electronic transitions occurring within their structures.

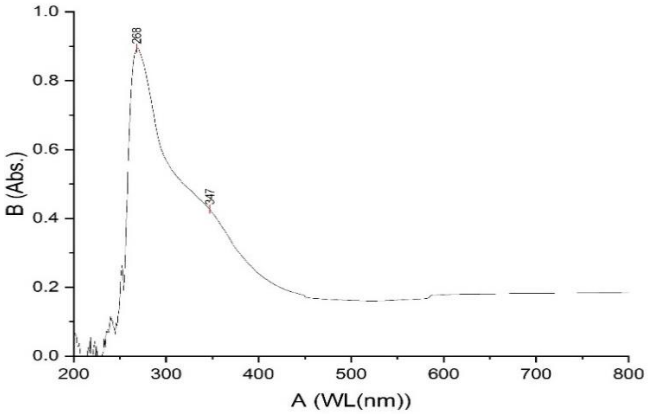

Fig. 3.2: UV of Iron nanoparticles synthesised from *Vernonia cineria*

3.5.2. FTIR

Result of FTIR of Vc- FeNPs (Fig 3.3) study showed sharp absorption peaks located at about 542.92, 1017.38, 1177.46, 1360.65, 1422.40, 2360.71, 2907.49, 3035.75, and 3525.63 cm^{-1}. These absorbance bands were known to be allied with the stretching vibrations for range of functional groups like R-Br (Alkyl halides), RCO-OH (Carboxylic acids), R-F (Alkyl halides), Ar2NH (Amines), C-C in ring (Aromatics), P-H phosphine (Misc), C=C-CO-OH (Carboxylic acids), Ar-H (Aromatics), RCH2OH (Alcohols) respectively (Table 3.4).

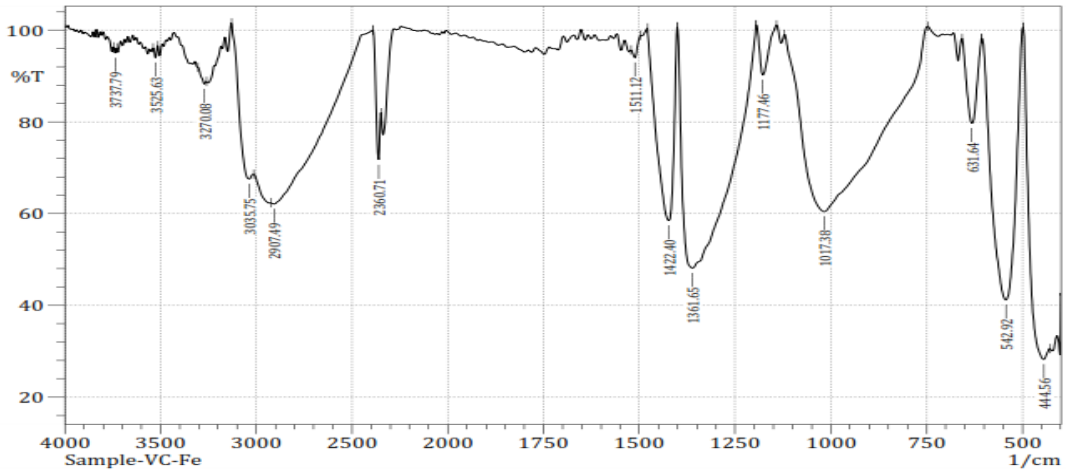

Fig 3.3 FTIR spectrum of iron nanoparticles extract of *V. cinerea*

Table 3.4. FTIR peak values and functional groups of FeNPs from *V. cinerea*

Wave length	Functional groups	Structure

Research Paper © 2012 IJFANS. All Rights Reserved, **UGC CARE Listed (Group -I) Journal**

444.56	Misc.	S-S disulfide
542.92	Alkyl halides	R-Br
1017.38	Carboxylic acids	RCO-OH
1177.46	Alkyl halides	R-F
1360.65	Amines	Ar2NH
1422.40	Aromatics	C-C in ring
1511.12	Misc.	N=O nitroso
2360.71	Misc.	P-H phosphine
2907.49	Carboxylic acids	C=C-CO-OH
3035.75	Aromatics	Ar-H
3525.63	Alcohols	RCH2OH
3737.79	Alcohols	R2CHOH

3.5.3. XRD

The XRD technique was used to determine and confirm the crystalline structure of synthesized iron nanoparticles. The XRD pattern of FeNPs synthesized using leaf extract of *V. cinerea* in Fig. 3.4. A number of strong braggs reflection with peaks were observed at specific angles at room temperature: 2θ value of 24.23°, 33.22°, 35.72°, 40.92°, 49.53°, 54.11°, 57.66°, 62.51°, and 64.04° respectively. The Scherrer relation was used in order to determine the crystallite size of the nanoparticles. This was accomplished by measuring the broadening of the XRD peaks of the preferred orientation. The average crystallite size was found to be 53nm.

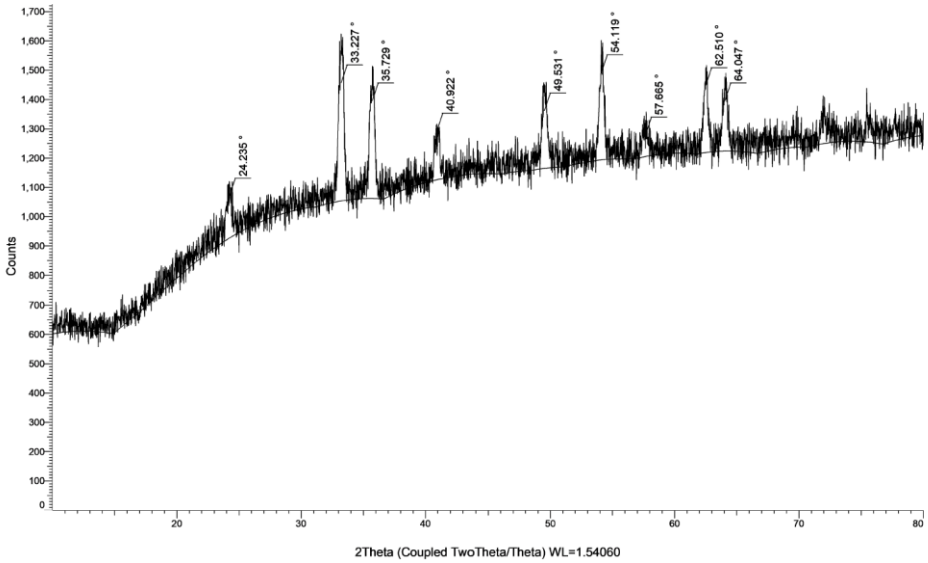

Fig. 3.4. XRD pattern of synthesized FeNPs from *V. cinerea*

3.5.4. Scanning Electron Microscopy and Energy-dispersive X-ray spectroscopy (EDX)

The surface morphology and size of the iron nanoparticles were analyzed by SEM. Based on the analysis of the SEM image, it can be observed that the nanoparticles exhibited a size distribution ranging from 1-5nm. Fig 3.5. showed that the particles are an agglomerated, irregular shape rough texture and smaller nanoparticles clustering. An EDAX examination is conducted to ascertain the

Research Paper © 2012 IJFANS. All Rights Reserved, **UGC CARE Listed (Group -I) Journal**

composition of iron oxide nanoparticles. EDAX analysis has shown the formation of pure iron oxide nanoparticles. The presence of elemental iron, potassium, chlorin, oxygen, sodium, aluminium and silicon in the extract of *V. cinerea* was confirmed by EDAX analysis (Fig 3.6).

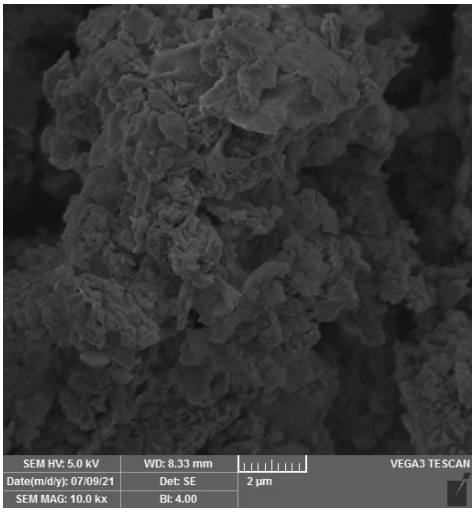

Fig. 3.5. SEM of iron nanoparticles from *V. cinerea*

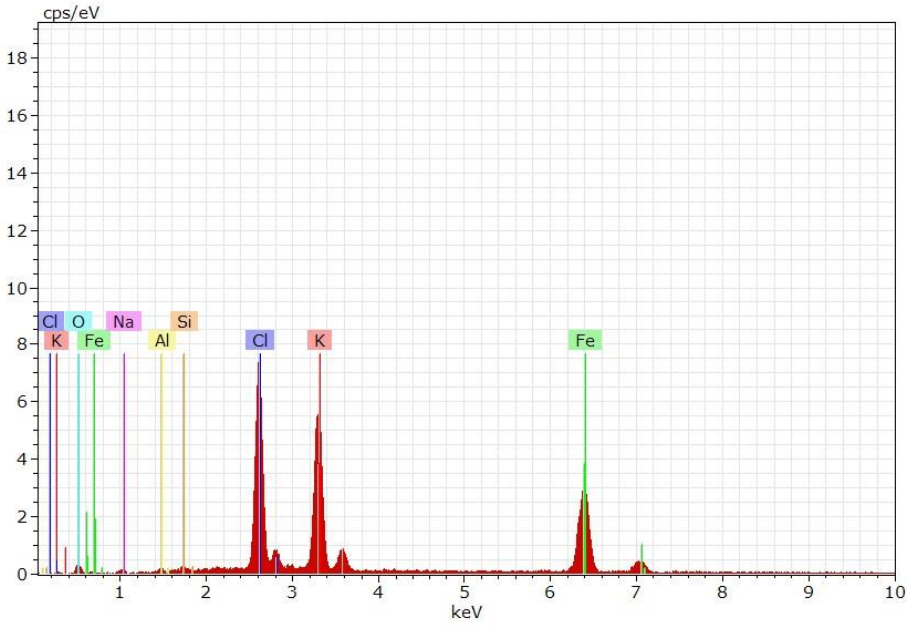

Fig. 3.6. EDAX of iron nanoparticles from *V. cinerea*

3.6. Anticancer activity

3.6.1. Anticancer activity against human lung cancer (A549) cell line

The anticancer activity of FeNPs derived from *V. cinerea* against human lung cancer (A549) cells observed to be concentration-dependent, as shown in Table 3.5 and Fig 3.7. Compared to the standard drug cisplatin, the results clearly demonstrated that increasing the concentration of nanoparticles led to a significant decrease in cell viability. At the lowest concentration of 12.5 µg/mL, *V. cinerea* iron nanoparticles reduced cell viability to 88.51%. As the nanoparticle concentration increased to 200 µg/mL, cell viability decreased significantly to 19.37%. Cytotoxicity gradually increased with increasing concentrations of FeNPs from 12.5µg/mL to 200µg/mL. Interestingly, the standard drug cisplatin treated A549 cell line exhibited a viability of 38.20% at a concentration of 20 µM. The IC_{50} values for *V. cinerea* FeNPs were determined to be 61.25µg/mL.

Table 3.5. Anti-cancer activity of *V. cinerea* FeNPs in comparison with the standard drug cisplatin against Human lung cancer (A549) cell line.

Concentrations µg/ml	Anticancer activity of human lung cancer (A549) cell line VC-FeNPs
12.5	88.51±0.0075
25	72.49±0.0095
50	55.09±0.018
100	39.67±0.006
200	19.37±0.017
Cisplatin(20µM)	38.20
IC_{50}	61.25

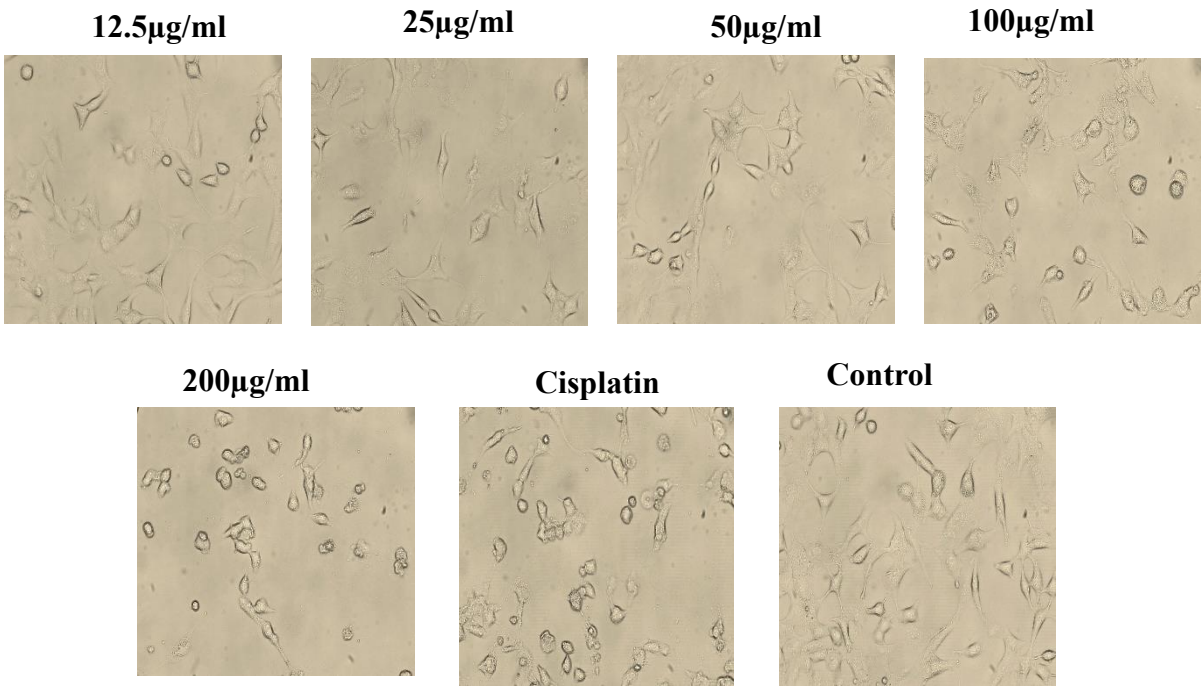

Fig 3.7. Cell viability of human lung cancer (A549) cell line treated with different concentrations of FeNPs derived from *V. cinerea*

3.6.2. Anticancer activity against human colon cancer (HCT-116) cell line

The anticancer activity of FeNPs derived from *V. cinerea* against human colon cancer (HCT-116) cells was observed to be concentration-dependent, as shown in Table 3.6 and Figure 3.7. Compared to the standard drug fluorouracil, the results clearly demonstrated that increasing the concentration of nanoparticles led to a significant decrease in cell viability. At the lowest concentration of 12.5 µg/mL, *V. cinerea* iron nanoparticles reduced cell viability to 63.43%. As the nanoparticle concentration increased to 200 µg/mL, cell viability decreased significantly to 18.20%. Interestingly, the standard drug fluorouracil treated HCT-116 cell line exhibited a viability of 48.49% at a concentration of 20 µM. The IC_{50} values for *V. cinerea* FeNPs were determined to be 28.49 µg/mL.

Table 3.6. Anti-cancer activity of *V. cinerea* FeNPs in comparison with the standard drug cisplatin against Human colon cancer (HCT-116) cell line.

Research Paper © 2012 IJFANS. All Rights Reserved, **UGC CARE Listed (Group -I) Journal**

Concentrations µg/ml	Anticancer activity of human colon cancer (HCT-116) cell line VC-FeNPs
12.5	63.43±0.012
25	52.29±0.019
50	40.61±0.004
100	29.66±0.115
200	18.20±0.012
Fluorouracil(20µM)	48.49
IC_{50}	28.49

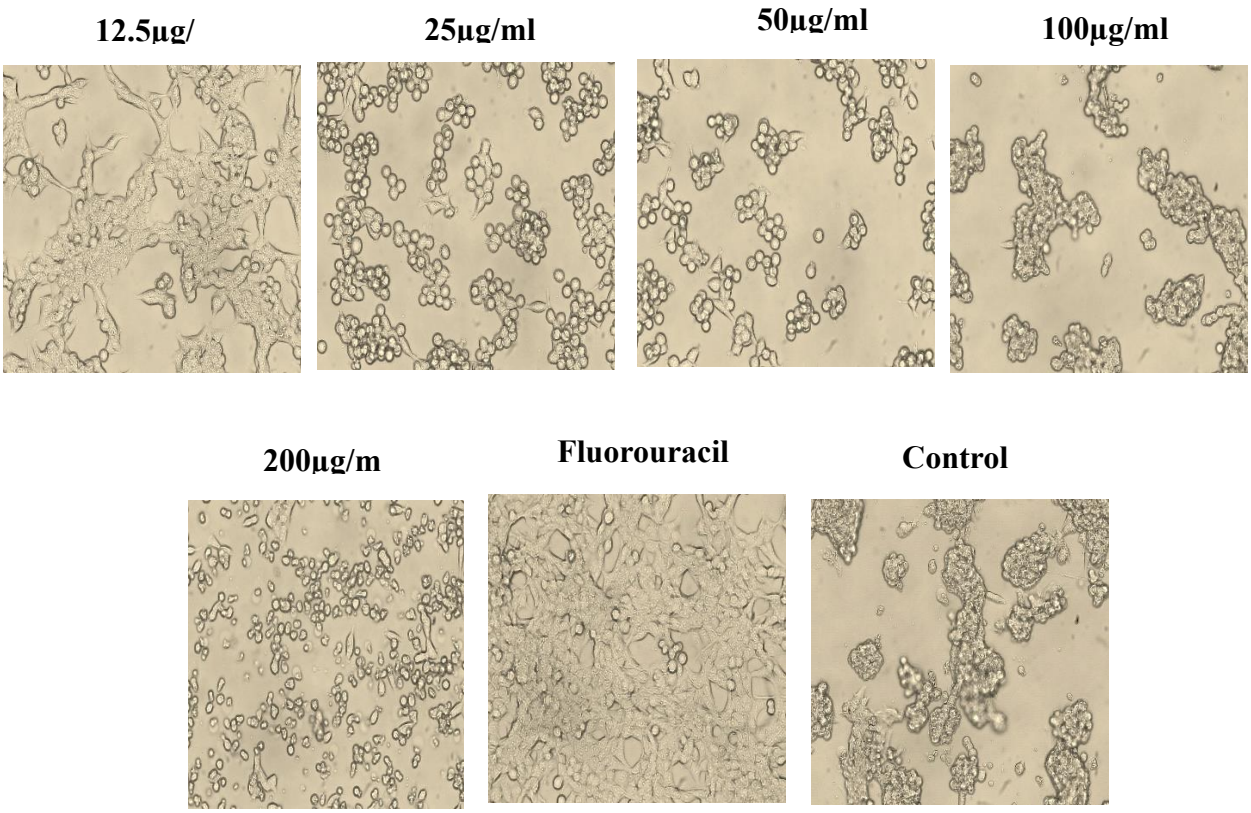

Fig 3.7. Cell viability of human colon cancer (HCT-116) cell line treated with different concentrations of FeNPs derived from *V. cinerea*

4. Discussion

The biological and environmentally friendly synthesis nano particles process is more efficient than the different physico-chemical procedures that are currently being used. It is possible to influence biological entities such as algae, fungi, bacteria, plants and so on. Using the biological/green technique, which is successful since it does not need the use of costly harmful chemicals or a significant amount of energy (Hussain *et al.*, 2016). This work exhibits the usage of leaf extract from *V. cinerea.* The antioxidant properties of plants are primarily due to their content of compounds that can serve as a helpful external antioxidant supply for living systems (Parveen et al., 2016). In the present study DPPH free radical scavenging activity of *V. cinerea* demonstrated significantly higher scavenging activities of 67.40%, 33.79%, and 72.67% for hexane, chloroform, and ethanol extracts, respectively. There is a correlation between the bioactive elements that have been found and the antioxidant activity (Goggi and Nutan, 2017). Goggi and Malpathak, (2017) reported that 54% DPPH radical scavenging activity for *V. cinerea* ethanolic leaf extract at a concentration of 100 µL. Sonibare et al. (2016) reported that *V. cinerea* hexane and chloroform extracts exhibiting the highest radical scavenging activities with IC_{50} values of 8.00 µg/mL and 8.63 µg/mL, respectively. Etim et al. (2015)

observed that *V. cinerea* exhibiting 17.30 µg/mL. 13.84% DPPH radical scavenging activity for *V. cinerea* methanolic extract at a concentration of 150 µg/mL. Goyal et al. (2017) observed that *V. cinerea* methanolic extracts exhibiting the highest radical scavenging activities with IC_{50} values of 429.94 µg/mL. Wannasetdecho et al (2022) reported that %RSA of 15.47% for *V. cinerea* hexane leaf extract. Alara et al (2018) reported that *V. cinerea* exhibiting the highest radical scavenging activities with IC_{50} values of 301.86 µg/mL. DPPH radical scavenging, *V. cinerea* ethanol extract demonstrated the strongest DPPH scavenging, followed by hexane and chloroform.

In the present study hydroxyl radical scavenging activity of *V. cinerea* leaf extracts was evaluated using hexane, chloroform and ethanol. At the highest concentration tested (300 µg/mL), exhibited scavenging activities of 35.09%, 33.56%, and 57.63%. Daffodil et al. (2014) observed that the IC_{50} values of 23.16µg/*ml for V. cinerea* against hydroxyl free radical scavenging activity. Rajamurugan et al. (2011) reported that the *V. cinerea* exhibiting the highest hydroxyl radical scavenging activities with IC_{50} values of 220 µg/m*l*. Hydroxyl radical scavenging was most potent *V. cinerea* hexane extract exhibited the strongest hydroxyl radical scavenging ability followed by chloroform, and then ethanol.

Superoxide anions are key players in the generation of reactive oxygen species (ROS) like hydrogen peroxide, hydroxyl radicals, and singlet oxygen. These ROS can cause significant oxidative damage to lipids, proteins, and DNA, leading to various cellular and tissue dysfunction (Pietta 2000). In the present study superoxide free radical scavenging activity of *V. cinerea* leaf extracts was evaluated using hexane, chloroform and ethanol. At the highest concentration tested (300 µg/mL), exhibited scavenging activities of 87.60%, 81.26%, and 6.06% Koksal et al. (2008) reported that 57.5 and 43.9 % superoxide free radical scavenging activity for *V. cinerea* water and ethanolic extracts. Goyal et al. (2017) reported that the IC_{50} values of 451.72 µg/ml for *V. cinerea* against superoxide free radical scavenging activity. Daffodil et al. (2014) observed that the IC_{50} values of 28.31µg/m*l for V. cinerea* against superoxide free radical scavenging activity. Sharma et al. (2017) reported that *V. cinerea* exhibiting the highest superoxide free radical scavenging activities with IC_{50} values of 451.72 µmol/g, respectively**.**

The green synthesis of iron nanoparticles using extracts of *V. cinerea* were successfully carried out. The colour changes of the solutions from green to dark brown indicated the reduction of Fe^{+3} ions in aqueous solution due to the excitation of surface plasmon vibrations in iron nanoparticles. The synthesis of nanoparticles has garnered the interest in the scientific community due to their numerous applications in optronic, sensing, catalysis and pharmaceuticals. Colour change in the synthesis of iron oxide nanoparticles using plant materials as reductant agents has been reported (Mirza et al., 2018). Metal nanoparticles exhibit a surface plasmon resonance phenomenon, leading to a distinctive absorption peak in the UV-Vis spectrum. This peak can be used to identify and analyze the properties of various metal nanoparticles. The UV spectra analysis of iron nanoparticles synthesized from *V. cinerea* extract revealed absorption peaks at 268nm. Fayyaz et al. (2022) observed that the peak at 264nm for FeNPs from *S. oleracea*. The broadness of the peak is a good indicator of the nanoparticle size.

FTIR spectral were used to identify the existence of functional groups associated with biologically synthesized nanoparticles. Vc- FeNPs absorption peaks located at about 542.92, 1017.38, 1177.46, 1360.65, 1422.40, 2360.71, 2907.49, 3035.75, 3270.08, and 3525.63 cm^{-1} suggested the presence of alkyl halides, carboxylic acids, amines, aromatics, misc, and alcohols. Ketones, aldehydes and carboxylic acids for zinc nanoparticles synthesized from *V. cinerea*, Azim et al. (2022) identified peaks aromatic, amines, and amino acid. According to the findings of the earlier investigations, which demonstrated the bands for O-H bonds and C=O bonds, the bands that were detected are consistent with those findings. The results of the FTIR analysis indicate that the organic functional groups that are present in the plant extract are likely responsible for stabilizing the iron nanoparticles that were generated from *V. cinerea* extract. FT-IR analysis confirmed that the bio reduction of ferric chloride into iron oxide nanoparticles are due to the reduction by capping material of *V. cinerea* leaf extract.

XRD is an essential technique for determining the characteristics of nanoparticles (NPs). Koteeswaran et al. (2019) reported that the XRD diffraction of *V. cinerea* silver nanoparticle had Bragg's reflections of 111, 200, 220 and 311 planes. Jara *et al.* (2024) reported that the iron nanoparticles synthesized with *Vernonia amygdalina* exhibit an irregular morphology and lack a uniform distribution in shape and size. Elemental composition of FeNPs synthesized using *V. cinerea* leaves extract was determined by using EDX analysis. It was observed that the percentage of iron is 30.88%, potassium is 26.56% and chlorine is 25.91% are high in FeNPs synthesized *V. cinerea.* Palei *et al.* (2023) also reported that EDAX of synthesized silver nanoparticle using the *V. cinerea* extracts. Scanning electron microscopy (SEM) was used to characterize the morphology of the nanoparticles. Sahayaraj et al. (2014) reported that the silver nanoparticle produced by *V. cinerea* were spherical in shape and particle size ranging from 5 to 50 nm as observed by SEM. Zani et al. (2016) reported that the silver nanoparticle produced by *V. cinerea* were spherical in shape and particle size ranging from 5.83nm-53.50nm. Sadek et al. (2022) reported that the *Botrytis cinerea* were spherical in shape. The synthesis of nanoparticles of *V. cinerea* leaf extracts was tested for its anticancer activity against A549 cells and HCT-116 cell lines. Similarly, Zani et al. (2016) reported that *V. cinerea*-AgNPs at a concentration of 31.25 mg/mL produced the highest cytotoxicity effects on Kasumi-1 cells after 72 hours. Palei et al. (2023) observed *in vitro* cytotoxicity activity of *V. cinerea* silver nanoparticles against neuroblastoma SHSY-5Y cell lines. Aboulthana et al. (2022) reported that green-synthesized silver nanoparticle using *Portulaca oleracea* exhibited maximum effect at 1000 µg/mL with an IC_{50} of 310.7 µg/mL in human colon cancer.

5. Conclusion

This study successfully demonstrated the potential of *V. cinerea* leaf extract as a green reducing and stabilizing agent for the synthesis of iron nanoparticles (FeNPs). The antioxidant properties of the leaf extract, comparable to standard ascorbic acid, were confirmed through various analyses. The formation of FeNPs was confirmed from UV visible spectroscopy, FTIR, XRD, SEM and EDAX analysis. The synthesized FeNPs exhibited promising anticancer activity against A549 and HCT-116 cell lines, indicating their potential as a novel therapeutic agent. The eco-friendly nature of the synthesis process, coupled with the multifunctional properties of the FeNPs, highlights their potential for diverse applications in biomedicine, environmental remediation, and catalysis. Further research is needed to optimize the synthesis process and characterize the FeNPs in detail., and evaluate their *in vivo* efficacy and toxicity profiles to fully realize their potential for sustainable nanotechnology.

References

1. **Okigbo, R. N., Anuagasi, C. L., & Amadi, J. E.** (2009). Advances in selected medicinal and aromatic plants indigenous to Africa. *Journal of Medicinal Plants Research*, 3(2), 86-95.
2. **Pankhurst, Q. A., Connolly, J., Jones, S. K., & Dobson, J.** (2003). Applications of magnetic nanoparticles in biomedicine. *Journal of Physics D: Applied Physics*, 36(13), R167. doi:10.1088/0022-3727/36/13/201.
3. **Gahlawat, G., & Choudhury, A. R.** (2019). A review on the biosynthesis of metal and metal salt nanoparticles by microbes. *RSC Advances*, 9(23), 12944-12967. doi:10.1039/C8RA10483B.
4. **Markides, H., Rotherham, M., & El Haj, A. J.** (2012). Biocompatibility and toxicity of magnetic nanoparticles in regenerative medicine. *Journal of Nanomaterials*, 2012, Article ID 614094. doi:10.1155/2012/614094.
5. **Vallabani, N. V. S., & Singh, S.** (2018). Recent advances and future prospects of iron oxide nanoparticles in biomedicine and diagnostics. *3 Biotech*, 8(6), 279. doi:10.1007/s13205-018-1219-7.
6. **Polyak, B., & Friedman, G.** (2009). Magnetic targeting for site-specific drug delivery: Applications and clinical potential. *Expert Opinion on Drug Delivery*, 6(1), 53-70. doi:10.1517/17425240802662795.

7. **Huang, H. S., & Hainfeld, J. F.** (2013). Intravenous magnetic nanoparticle cancer hyperthermia. *International Journal of Nanomedicine*, 8, 2521-2532. doi:10.2147/IJN.S43770.
8. **Zhao, C., Qiao, Y., Jonsson, P., Wang, J., Xu, L., Rouhi, P., Sinha, I., Cao, Y., Williams, C., & Dahlman-Wright, K.** (2014). Genome-wide profiling of AP-1–regulated transcription provides insights into the invasiveness of triple-negative breast cancer. *Cancer Research*, 74(14), 3983-3994. doi:10.1158/0008-5472.CAN-14-1034.
9. **Noruzi, M.** (2015). Biosynthesis of gold nanoparticles using plant extracts. *Bioprocess and Biosystems Engineering*, 38(1), 1-14. doi:10.1007/s00449-014-1251-1.
10. **Rokade, H. M., et al.** (2018). Review on nanobiotechnology applications in medicine. *International Journal of Current Pharmaceutical Research*, 10(4), 1-5. doi:10.1016/j.nano.2018.06.005.
11. **Ramanathan, A. A., & Aqra, M. W.** (2019). An overview of the green road to the synthesis of nanoparticles. *Journal of Materials Science Research and Reviews*, 2(1), 114-124. doi:10.9734/jmsrr/2019/v2i130059
12. **Khare, C. P.** (2007). Indian Medicinal Plants: An Illustrated Dictionary. *New York: Springer Science & Business Media.*
13. **Kuo, M.** (2003). Interaction and customer satisfaction in online community service quality. *International Journal of Service Industry Management*, 14(4), 426-442.
14. **Prajapati, N. D., Purohit, S. S., Sharma, A. K., & Kumar, T.** (2003). Agro's Dictionary of Medicinal Plants.*Jodhpur: Agrobios (India).*
15. **Ansar, S., Alshehri, S. M., Abudawood, M., Hamed, S. S., & Ahamad, T**. (2017). Antioxidant and hepatoprotective role of selenium against silver nanoparticles. *International journal of nanomedicine*, 7789-7797.
16. **Krishnan, S. N., Talari, D., Rajangam, J., Pujari, L., Palei, N. N., Balaji, A., & Surendran, V.** (2021). Protective effect of *Vernonia cinerea* against sunset yellow induced anxiogenic behaviour in mice model: Counteract oxidative damage based approach. *The Natural Products Journal*, *11*(4), 537-545.
17. **Gupta, R., Gigras, P., Mohapatra, H., Goswami, V. K., & Chauhan, B.** (2003). Microbial α-amylases: a biotechnological perspective. *Process biochemistry*, *38*(11), 1599-1616.
18. **Pratheeshkumar, Poyil & Kuttan, G.** (2012). Antimetastatic potential of vernolide-A, a sesquiterpenoid from *Vernonia cinerea* L. *Human & experimental toxicology*. 31. 66-80.
19. Divya Theja, D **&** Nirmala, S. (2023). A review of *Vernonia cinerea* L. ethno-medicinal uses and pharmacology shows that it could be a useful plant for medical purposes. *Intelligent Pharmacy*.
20. **Palei, N. N., Krishnan, S. N., Jayaraman, R., Reddy, S. H., Balaji, A., Samanta, M. K., & Mohanta, B. C.** (2023). Green Synthesis of Silver Nanoparticles of *Vernonia cinerea* Leaf Extract and their In vitro Cytotoxicity Activity against Neuroblastoma SHSY-5Y Cell Lines, Antimicrobial and Antioxidant Studies. Recent patents on nanotechnology, 17(3), 270–280.
21. **Hussain, S., Khan, F., Cao, W., Wu, L., & Geng, M. (2016).** Seed priming alters the production and detoxification of reactive oxygen intermediates in rice seedlings grown under sub-optimal temperature and nutrient supply. *Frontiers in plant science*, *7*, 439.
22. **Parveen, K., Banse, V., & Ledwani, L.** (2016). Green synthesis of nanoparticles: Their advantages and disadvantages. In *AIP conference proceedings*, Vol. 1724, No. 1.
23. **Goggi, A. G., & Nutan Malpathak, N. M.** (2017). Antioxidant activities of root, stem and leaves of Vernonia cinerea (L) Less.178-183.
24. **Sonibare, M. A., Aremu, O. T., & Okorie, P. N.** (2016). Antioxidant and antimicrobial activities of solvent fractions of Vernonia cinerea (L.) Less leaf extract. *African health sciences*, *16*(2), 629-639.

25. **Etim, E., Aniefiok Udobre, Anwanabasi Udoh, Emem Ed**. (2015). Evaluation of the antioxidant property of Vernonia Cinerea (L.) LESS. (Asteraceae) using 2.2- Diphenyl-1- Picrylhydrazine (DPPH) Assay Method. *The Pharma Innovation Journal*; 4(6): 10-14
26. **Wannasetdecho, T., Sonklin, C., Pranee, S., & Seeyangnok, S**. (2022). Chemical Constituents of Vernonia cinerea (L.) Less and Their Antioxidant Activity. *Journal of Food Science and Agricultural Technology (JFAT)*, *6*(1), 25-29.
27. **Rajamurugan, R., Selvaganabathy, N., Kumaravel, S., Ramamurthy, C. H., Sujatha, V., Suresh Kumar, M., & Thirunavukkarasu, C.** (2011). Identification, quantification of bioactive constituents, evaluation of antioxidant and *in vivo* acute toxicity property from the methanol extract of Vernonia cinerea leaf extract. *Pharmaceutical biology*, *49*(12), 1311-1320.
28. **Pietta. PG.,** (2000). Flavonoids as Antioxidants. *Journal of Natural Products* 2000 *63* (7), 1035-1042.
29. **Koksal, F., Altun, F., Yiğit, İ., Şahin, Y.,** (2008). Combined effect of silica fume and steel fiber on the mechanical properties of high strength concretes. *Constr. Build. Mater*. 22, 1874-1880.
30. **Goyal, P. K., Verma, S. K., & Sharma, A. K.** (2017). Quantification of total phenolic and flavonoid contents, and evaluation of free radical scavenging potential of Vernonia cinerea. *Asian Pacific Journal of Health Sciences*, 279-287.
31. **Daffodil, D. A., Lincy, Packia & Mohan, Veerabah**u. (2014). Study of whole plant of vernonia cinerea less. for in vitro antioxidant activity. *International Journal of Pharmacy*. 4. 172-178.
32. **Mirza, A. U., Kareem, A., Nami, S. A., Khan, M. S., Rehman, S., Bhat, S. A., et al.** (2018). Biogenic Synthesis of Iron Oxide Nanoparticles Using Agrewia Optiva and Prunus Persica Phyto Species: Characterization, Antibacterial and Antioxidant Activity. *J. Photochem. Photobiol. B: Biol.* 185, 262–274.
33. **Fayyaz, B., Zahra, M. B., & Haider, M. S.** (2022). Screening of Phenolic Compounds from Spinach (Spinacia oleracea), Green Synthesis of Iron-Nanoparticles and Determination of its Anti-Microbial Effect on Escherichia coli.
34. **Zeba Azim, N.B. Singh, Shubhra Khare, Ajey Singh, Nimisha Amist, Niharika & Ravi Kumar Yadav**, (2022). Green synthesis of zinc oxide nanoparticles using Vernonia cinerea leaf extract and evaluation as nano-nutrient on the growth and development of tomato seedling, *Plant Nano Biology*, Vol. 2, 100011.
35. **Jara, Y.S., Mekiso, T.T. & Washe, A.P.** (2024). Highly efficient catalytic degradation of organic dyes using iron nanoparticles synthesized with *Vernonia Amygdalina* leaf extract. *Sci Rep* 14, 6997.
36. Sahayaraj, Kitherian., Sathiyamoorthy, Rajesh., Roobadevi, M & Azizi, Susan. (2014).*Vernonia cinerea* (L.) Less. silver nanocomposite and its antibacterial activity against a cotton pathogen. *Research on Chemical Intermediates*. 41. 10.1007/s11164-014-1676-8.
37. **Sadek ME, Shabana YM, Sayed-Ahmed K, & Abou Tabl AH.** (2022). Antifungal Activities of Sulfur and Copper Nanoparticles against Cucumber Postharvest Diseases Caused by Botrytis cinerea and Sclerotinia sclerotiorum. *Journal of Fungi*. 8(4):412.
38. **Zani, R.A., Ahmad, N.H., & Razak, S.N.** (2016). synthesis and characterisation of silver nanoparticles using vernonia cinerea aqueous extract and their cytotoxicity activity against kasumi-1 cell line.pa
39. **Aboulthana, W.M., El-Sayed Ibrahim, N., Mohamed Osman, N., Mahmoud Seif, M., Amgad Kamal Hassan, Ahmed Mahmoud Youssef, Amal Mostafa El-Feky, & Madboli, A. A**. (2022) Evaluation of the Biological Efficiency of Silver Nanoparticles Biosynthesized Using Croton tiglium L. Seeds Extract against Azoxymethane Induced Colon Cancer in Rats.. *Asian pacific Journal of Cancer prevention.*